Title
Spermine Block of the Strong Inward Rectifier Potassium Channel Kir2.1

Journal
The Journal of General Physiology, 120(1)

ISSN
0022-1295

Authors
Xie, Lai-Hua
John, Scott A
Weiss, James N

Publication Date
2002-07-01

DOI
10.1085/jgp.20028576

Peer reviewed

Spermine Block of the Strong Inward Rectifier Potassium Channel Kir2.1: Dual Roles of Surface Charge Screening and Pore Block

Lai-Hua Xie, Scott A. John, and James N. Weiss

Cardiovascular Research Laboratory, Departments of Medicine (Cardiology) and Physiology, University of California at Los Angeles, School of Medicine, Los Angeles, CA 90095

ABSTRACT Inward rectification in strong inward rectifiers such as Kir2.1 is attributed to voltage-dependent block by intracellular polyamines and Mg^{2+}. Block by the polyamine spermine has a complex voltage dependence with shallow and steep components and complex concentration dependence. To understand the mechanism, we measured macroscopic Kir2.1 currents in excised inside-out giant patches from *Xenopus* oocytes expressing Kir2.1, and single channel currents in the inside-out patches from COS7 cells transfected with Kir2.1. We found that as spermine concentration or voltage increased, the shallow voltage-dependent component of spermine block at more negative voltages was caused by progressive reduction in the single channel current amplitude, without a decrease in open probability. We attributed this effect to spermine screening negative surface charges involving E224 and E299 near the inner vestibule of the channel, thereby reducing K ion permeation rate. This idea was further supported by experiments in which increasing ionic strength also decreased Kir2.1 single channel amplitude, and by mutagenesis experiments showing that this component of spermine block decreased when E224 and E299, but not D172, were neutralized. The steep voltage-dependent component of block at more depolarized voltages was attributed to spermine migrating deeper into the pore and causing fast open channel block. A quantitative model incorporating both features showed excellent agreement with the steady-state and kinetic data. In addition, this model accounts for previously described substate behavior induced by a variety of Kir2.1 channel blockers.

KEY WORDS: K^+ channels • inward rectification • polyamine • spermine • modeling

INTRODUCTION

Inward rectifier potassium (Kir) channels conduct inward current efficiently at potentials negative to the K^+ reversal potential (E_K), but progressively less so as membrane potential approaches or exceeds E_K. The inward rectifying property plays an essential role in stabilizing resting membrane potential and regulating excitability in many cell types (Hille, 2001; Doupnik et al., 1995).

For strong inward rectifiers in the Kir2 family, the mechanism underlying strong inward rectification involves voltage-dependent block by Mg^{2+} and polyamines (Matsuda et al., 1987; Vandenberg, 1987; Ficker et al., 1994; Lopatin et al., 1994; Fakler et al., 1995). Mutagenesis studies have identified negatively charged residues in two different regions which are critical for strong inward rectification: D172 in the M_2 region (Lu and MacKinnon, 1994; Stanfield et al., 1994; Wible et al., 1994; Yang et al., 1995) and E224 and E299 in the cytoplasmic COOH terminus (Taglialatela et al., 1995; Yang et al., 1995; Kubo and Murata, 2001).

Block by polyamines has a complex dependence on both voltage and concentration. A quantitative model of polyamine block has been described by Lopatin et al. (1995). In their "long-pore plugging" model, they assumed two spermine molecules sequentially enter the channel pore. The model reproduced the shallow voltage-dependent component of block with rapid kinetics due to the first spermine entering the pore, and the steeply voltage-dependent component of block with slower kinetics corresponding to a second spermine molecule entering the pore and interacting with the first spermine molecule. Subsequently, they were able to simplify the model somewhat by postulating that some of the steep voltage dependence was related to polyamines sweeping K^+ ions from the pore (Pearson and Nichols, 1998). In a previous study, we performed competition experiments using the polyamine toxin philanthotoxin, which structurally resembles polyamine at one end, but has a large hydrophobic group at the other end (Lee et al., 1999). The results, as well as those of a recent study by Kubo and Murata (2001), suggested a model in which positively charged polyamines such as spermine can bind to a region of the channel involving the negatively charged residues E224 and E299 without occluding the pore. Kubo and Murata (2001) argued that the two negative charges function as an intermediate binding site for spermine near the inner vestibule, which then facilitates entry of spermine to a binding site occluding ion permeation lo-

Address correspondence to James N. Weiss, Division of Cardiology, Rm. 3645, MRL Building, UCLA School of Medicine, Los Angeles, CA 90095. Fax: (310) 206-5777; E-mail: jweiss@mednet.ucla.edu

cated deeper in the pore at D172. An important point shared in both our and Kubo's models is that the channel exhibits a second open state when spermine binds to E224 and/or E299.

In the present study, we have extended the analysis of spermine block in Kir2.1 channels and, based on the findings, propose a new model which accounts for the complex voltage and concentration dependence and kinetics at both the macroscopic and single channel levels. This model is built on the previous idea that positively charged polyamines such as spermine interact with negatively charged moieties (specifically E224 and E299) near the inner vestibule of the channel. The novel feature is that this interaction screens this local negative surface charges, which normally serve to maximize the rate of K ion permeation (single channel conductance) through the pore. Thus, we attribute the component of spermine block with shallow voltage dependence to a charge-screening effect near the inner vestibule that reduces single channel conductance. The steep voltage-dependent component remains attributed to movement of spermine from these nonocclusive sites to an occlusive site deep in the pore (at D172). This interpretation is supported by single channel studies documenting that spermine, as well as ionic strength, reduces single channel conductance through Kir2.1 channels, and by mutagenesis experiments in which neutralization of the putative inner vestibule negative surface charges at E224 and E229, but not the pore-lining residue D172, attenuates the effects of surface charge screening effects of spermine. In addition to providing an excellent quantitative fit to the complex voltage and concentration of spermine block, this model can explain previously described substate behavior induced by a variety of Kir2.1 channel blockers.

MATERIALS AND METHODS

Molecular Biology and Preparation of Oocytes

The Kir2.1 cDNA (Kubo et al., 1993) was provided by Dr. Lily Y. Jan (University of California at San Francisco, San Francisco, CA). PCR mutagenesis was performed by the overlap extension technique (Ho et al., 1989) to generate the Kir 2.1 mutants. cRNAs were synthesized using T7 polymerase (Ambion) and injected into stage IV-V *Xenopus* oocytes.

Oocytes were isolated by partial ovariectomy from mature female *Xenopus* anesthetized with 0.1% tricaine. They were then defolliculated by treatment for 1 h with 1 mg/ml collagenase (TypeII; Life Technologies) in Barth's solution containing (mM): 88 NaCl, 1 KCl, 2.4 $NaHCO_3$, 0.3 $Ca(NO_3)_2{\cdot}4H_2O$, 0.41 $CaCl_2$, 0.82 $MgSO_4$, 15 HEPES, and 50 mg/ml gentamicin, 10 mg/ml Baytril; pH 7.6. The day after collagenase treatment, selected oocytes were pressure-injected with ~50 nl RNA (1–100 ng/ml). Oocytes were maintained at 18°C in Barth's solution and electrophysiological studies were conducted 1–3 d later. Immediately before recording, each oocyte was incubated in a hypertonic solution containing (mM): 90 KCl, 4 $MgCl_2$, 5 HEPES, 200 sucrose, pH 7.4 for ~10 min, and the vitelline membrane was removed before patching the oocyte.

Functional Expression in COS7 Cells

cDNAs of Kir2.1 (0.8 μg) and green fluorescent protein (GFP) (0.2 μg) were cotransfected into COS7 cells using GenePORTER 2 transfection reagent (Gene Therapy Systems). COS7 cells were cultured in Dulbecco's modified Eagle's medium supplemented with 10% (vol/vol) fetal bovine serum. Experiments were performed on the GFP-positive cells ~24–48 h after transfection.

Electrophysiology and Data Analysis

Macroscopic currents recording from oocytes. Membrane currents were recorded from excised inside-out giant patches from injected oocytes with an Axopatch 200A amplifier (Axon Instruments, Inc.) at room temperature, as described previously (Shieh et al., 1996). Patch electrodes were pulled from thin-wall borosilicate glass (Garner Glass Co.) and had a tip diameter of 20–30 μm after fire polishing. The patch electrode solution contained: 85 KCl, 1.8 $CaCl_2$, 5 K_2HPO_4, 5 KH_2PO_4 to pH 7.4 with KOH. The standard bath solution contained (mM): 75 KCl, 5 K_2EDTA, 5 K_2HPO_4, 5 KH_2PO_4, pH 7.2 with KOH. The total $[K^+]$ in the pipette solution and bath solution was ~100 mM in most of the experiments. In the experiments testing the effect of ionic strength on surface charge screening, the pipette solution contained 15 KCl, 140 sucrose, 1.8 $CaCl_2$, 5 K_2HPO_4, 5 KH_2PO_4 to pH 7.4 with KOH; the bath solution contained 15 KCl, 5 EDTA, 5 K_2HPO_4, 5 KH_2PO_4 with 140 sucrose in control, 70 N-Methyl-D-Glucamine (NMG) or NaCl in the test solution. TEA, spermine, or spermidine were added to the bath solution with pH readjusted to the desired level. Chemicals were purchased from Sigma-Aldrich. Current through Kir2.1 channels was measured by subtracting the current recorded in 30 mM TEA solution from the total measured current. Data were filtered with an 8-pole Bessel filter (Frequency Devices) at 1 kHz and digitized at 2 kHz via a DigiData 1200 interface (Axon Instruments, Inc.). Data acquisition and analysis were performed using pCLAMP 6 or 7 software (Axon Instruments, Inc.).

Single channel recording from COS7 cells. Membrane currents were recorded at room temperature from inside-out patches excised from transfected COS7 cells, using an Axopatch 200B amplifier (Axon Instruments, Inc.). Patch electrodes were pulled from thick-wall borosilicate glass (Warner Instrument Corp.) and had a resistance of 5–8 MΩ when filled with the pipette solution. Electrodes were coated near their tips with sylgard (Dow Corning Co.) or *N,N*-dimethyltrimethylsilylamine (Fluka) to reduce electrical capacitance. The total $[K^+]$ in the pipette solution and bath solution were 140 mM. Data were filtered at 5 kHz and digitized at 10 kHz if not otherwise indicated.

All experiments were conducted at room temperature (20–24°C). Modeling and curve fitting was performed using a commercially available simulation package (Scop 3.5; Simulation Resource, Inc.).

RESULTS

Inward Rectification of Macroscopic Kir2.1 Currents in Cell-attached Patches Versus Excised Inside-Out Patches

Fig. 1 A shows typical currents from Kir2.1 channels expressed in *Xenopus* oocytes recorded from a cell-attached patch. As the test voltage was stepped from 40 mV to more negative potentials, the amplitude of inward currents increased gradually with hyperpolarization, whereas little or no current was detected at test potentials greater than −20 mV (Fig. 1 A, left). The quasi-

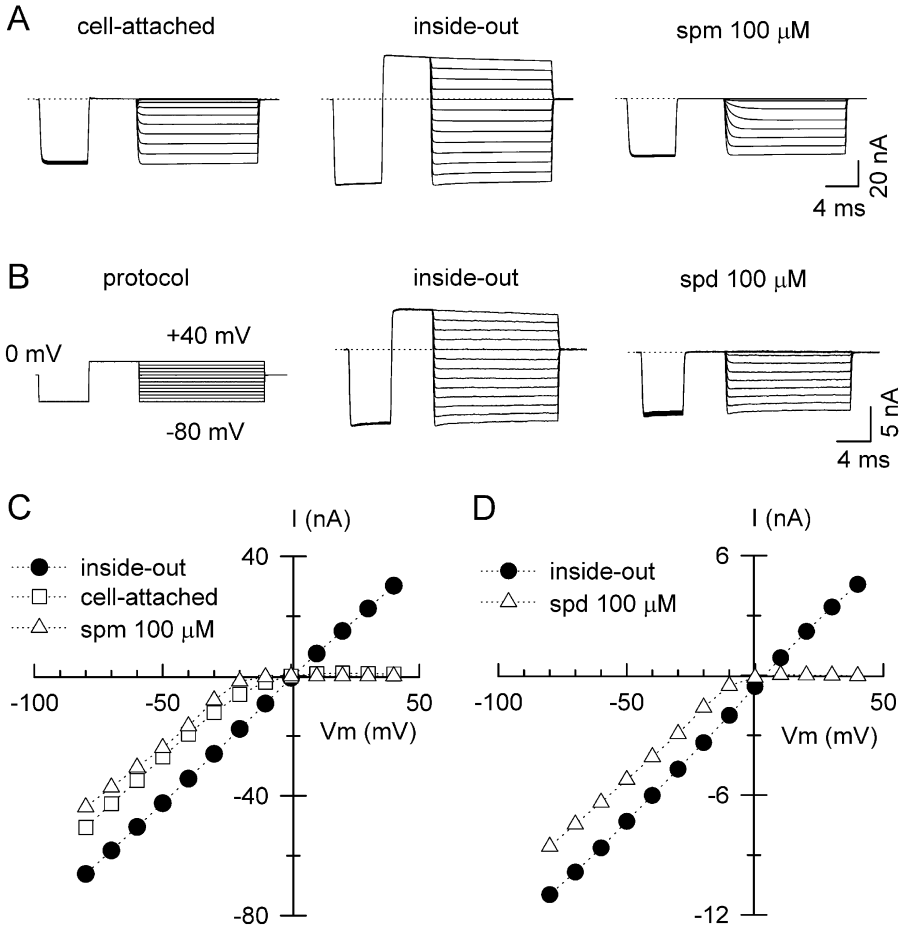

FIGURE 1. Inward rectification of Kir2.1 current in cell-attached patch versus inside-out patch. (A) Currents were recorded from *Xenopus* oocytes injected with Kir2.1 mRNA in the cell-attached patch configuration (left) and following excision as an inside-out patch in the absence (middle) or presence of 100 μM spermine (right). (B) Currents recorded from a different patch in the absence (middle) and presence (right) of 100 μM spermidine. The voltage clamp protocol is shown in the left panel of B. The dotted lines indicate the zero current level. (C) I-V curves of the steady-state current at the end of the test pulses in A. (D) I-V curve of the steady-state current at the end of the test pulse in B. Note the similar shapes of the I-V curve for the cell-attached patch and the excised inside-out patch with 100 μM spermine or spermidine present.

steady-state I-V relationship at the end of the 15 ms pulses (Fig. 1 C, open squares) shows a typical inward rectification pattern of the strong inwardly rectifying K channels. Note that the extrapolation of the linear region of the inward current conductance intersects the voltage axis well below E_K (= 0 mV), reflecting the strong voltage dependence of the blocking mechanism.

After excision into Mg^{2+} and polyamine-free solution, both inward and outward currents increased gradually with time and reached a steady-state level ~5 min after excision, with the steady-state I-V relationship becoming linear in both inward and outward directions (Fig. 1, A and B, middle; Fig. 1, C and D, closed circles). The loss of the inward rectification in inside-out patches has been shown to be a result of the washout of blocking particles such as polyamines (Lopatin et al., 1994) and Mg^{2+} (Matsuda et al., 1987) from the cytoplasmic surface of the patch. Strong inward rectification was restored by adding 100 μM spermine (Fig. 1 A, right) or spermidine (Fig. 1 B, right) to the bath (cytoplasmic) solution, approximately reproducing the I-V curve for the cell-attached patch (Fig. 1, C and D, open triangles). Slower activation of inward currents with spermine reflects its slower unblocking rate compared with spermidine and to other blocking particles (Mg^{2+} and other polyamines) present in the cell-attached patch configuration. However, aside from these subtle differences, the addition of spermine or spermidine reconstitutes the major features of inward rectification present in the channels in their natural environment. Since spermine's slower unblocking kinetics lends itself more readily to quantitative analysis, subsequent experiments were focused on spermine.

Block of Macroscopic Kir2.1 Current by Physiological Concentrations of Spermine

Fig. 2 shows the blocking effects of spermine over a physiological concentration range in an excised inside-out patch, after washing for ~5 min until the I-V relation had become almost linear (Fig. 2 A, control). The currents were measured during depolarizing pulses (−100–40 mV) after a 5 ms prepulse to −100 mV. Two representative sets of the current traces after application of 1 and 100 μM spermine are shown in Fig. 2 A. The quasi-steady-state I-V relationships in the absence and presence of 1, 10, 100, and 1,000 μM spermine are plotted in Fig. 2 B. To better illustrate the component of block attributable to spermine at each voltage, steady-state current (I) for the different

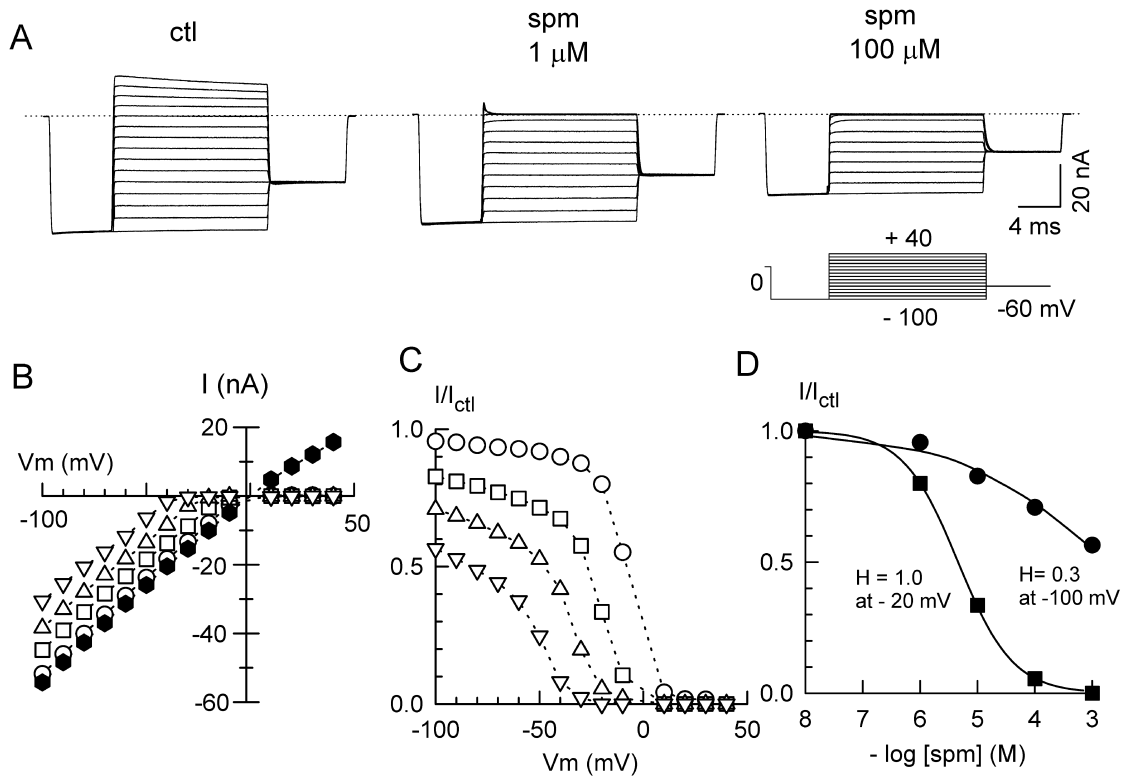

FIGURE 2. Macroscopic I-V relationship for different concentration of spermine. (A) Representative current traces recorded from inside-out patch in the presence of 0 (control), 1, and 100 μM spermine. The dotted line indicates the zero current level. Voltage protocol is shown at the bottom. (B) Steady-state I-V curves for control (●), and 1 μM (○), 10 μM (□), 100 μM (△) and 1 mM (▽) spermine. (C) The ratio of the steady-state current (I) in the presence of spermine to that in its absence (I_{ctl}) plotted against voltage, for the spermine concentrations in B (with corresponding symbols). (D) Comparison of the concentration dependence of the spermine block at −100 mV (●) and −20 mV (■), respectively, from the experimental data in C. Solid lines are best fits to a Hill equation: $I/I_{ctl} = 1/(1 + ([spm]/K_d)^H)$, where K_d is spermine concentration causing half-maximal block and H is the Hill coefficient. The values of H at −100 and −20 mV are as indicated.

spermine concentrations was normalized to the corresponding current in the absence of spermine (I_{ctl}) in Fig. 2 C.

Fig. 2 C clearly reveals two components of block. At 100 μM spermine, for example, a shallow weakly voltage-dependent block of 40–50% persists at potentials more negative than −60 mV, whereas a strongly voltage-dependent component of block develops at potentials positive to −60 mV. The concentration dependence of spermine block at −100 and −20 mV is compared in Fig. 2 D. The spermine concentration causing half-maximal block was 1.8 mM at −100 mV and 4.7 μM at −20 mV, with Hill coefficients of 0.3 and 1, respectively. Unless allosteric effects are invoked, this low value of the Hill coefficient at −100 mV cannot be explained by a reaction scheme comprised solely of fully open and fully closed states. However, it could be accounted for if spermine induced partially conductive (subconductance) states at very negative potentials, analogous to the previously described effects of certain cations (Mg^{2+}, Ca^{2+}) (Matsuda et al, 1989; Mazzanti et al., 1996). To investigate this possibility, we performed single channel recordings to examine the effects of spermine on single channel conductance.

Spermine Reduces Single Channel Amplitude Progressively as Membrane Voltage Depolarizes

Fig. 3 shows representative single channel currents recorded in inside-out patches excised from COS7 cells expressing Kir2.1. At −60 mV, increasing spermine concentration from 0.1 to 1 mM had no significant effect on channel open probability (P_o = 0.95 ± 0.17, 0.93 ± 0.21, and 0.91 ± 0.26 at 0, 0.1, and 1 mM spermine, respectively, n = 3 patches), despite the fact that these same spermine concentrations significantly reduced the macroscopic current amplitude at −60 mV (Fig. 2). Rather than suppressing current by decreasing open probability, spermine progressively reduced the single channel current amplitude at −60 mV as its concentration increased from 2.00 ± 0.04 to 1.40 ± 0.04 and 1.05 ± 0.06 pA with 0, 0.1, and 1 mM spermine re-

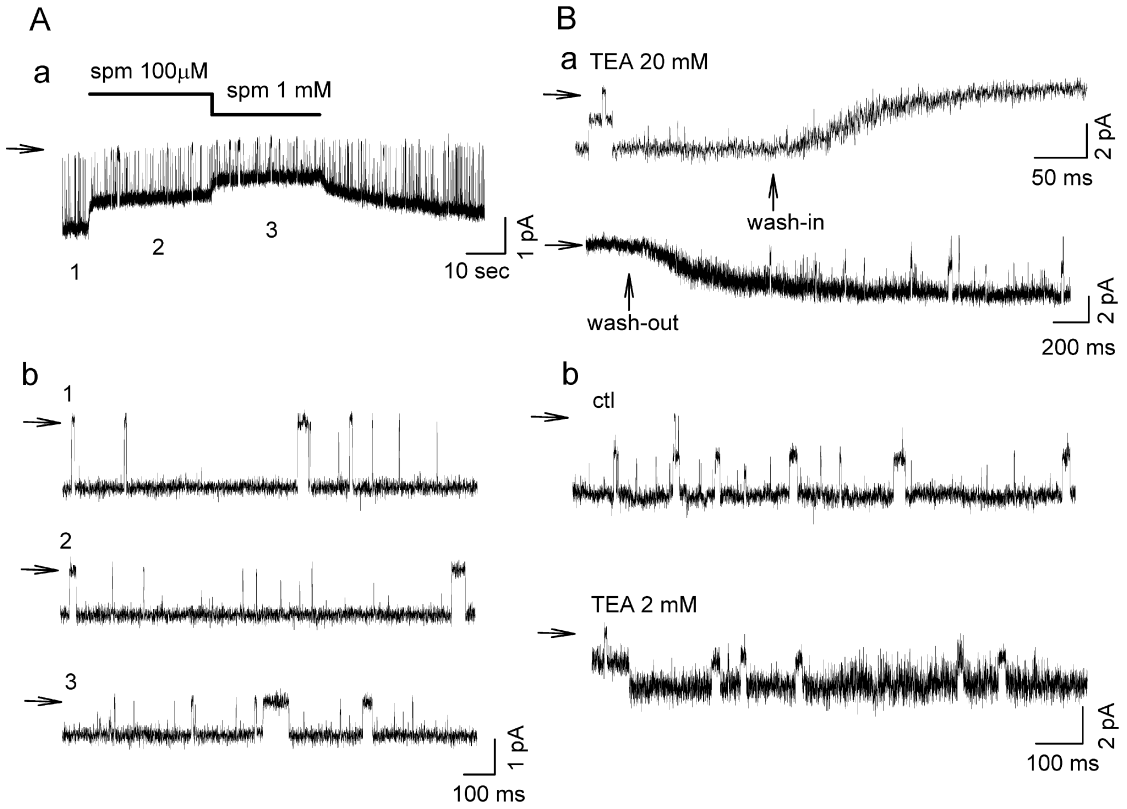

FIGURE 3. Effect of spermine and TEA on Kir2.1 single channel currents, recorded from inside-out patches excised from COS7 cell transfected with Kir2.1 cDNA (holding potential of −60 mV). (A a) Application of 100 μM and 1 mM spermine reduced single channel amplitude. The continuous change of the single channel amplitude is particularly evident during the wash-out phase. The expanded traces in b, 1 and 2, are from the corresponding times in A a labeled 1, 2, and 3. (B) Blocking effect of TEA on single Kir2.1 channel currents. With 20 mM TEA, note the increase in open channel noise during the wash-in and washout of TEA (trace a). For 2 mM TEA (2 mM) at steady-state (trace b), the unitary amplitude is reduced but the open channel noise is increased. Zero current levels are indicated by horizontal arrows.

spectively (n = 4 patches). In addition, the changes in single channel current amplitude did not occur in resolvable discrete steps during the wash-in and wash-out of spermine (Fig. 3 A, a). As is especially clear during spermine washout, the single channel amplitude increased progressively and without any obvious change in the level of open channel noise.

The decrease in single channel amplitude could not be attributed to spermine causing kinetically unresolved rapid open channel block, resulting in an apparent reduction in single channel current (as an artifact of limited bandwidth of the amplifier). As shown in Fig. 3 B, TEA, which has much faster apparent blocking and unblocking kinetics (compare the time course of TEA washout in Fig. 3 B with spermine washout in Fig. 3 A), clearly increased the level of open channel noise during wash-in and wash-out of 20 mM TEA (Fig. 3 B, a) or during steady-state application of 2 mM TEA (Fig. 3 B, b). Since the digitization rate (10 kHz) and filter settings (5 kHz) in the traces in Fig. 3, A and B, were identical, unresolved rapid open channel block by spermine, with its slower kinetics, should have shown a greater increase in open channel noise than TEA, but this was not observed. If the assumption that spermine blocking kinetics are much slower than TEA kinetics is valid, this observation effectively excludes unresolved fast open channel block as the mechanism of reduction in single channel amplitude by spermine.

Fig. 4 A provides further support that the reduction in single channel amplitude was not due to unresolved fast open channel block. In this experiment, single channel currents were recorded from an excised inside-out patch in which spermine concentration (1 mM) remained constant during a voltage ramp from −100 to 0 mV at 200 mV/s. Two channels were active in the patch. Under control conditions, the I-V curve during the voltage ramp was linear with a slope conductance of ~35 pS, and reversed at E_K = 0 mV. In the presence of 1 mM spermine, the I-V curve recapitulated the appearance of the macroscopic I-V curve in Fig. 2 B. At voltages negative to −50 mV, the single channel current amplitude was reduced in a voltage-dependent manner, and the level of open channel noise was unchanged by spermine. At voltages more positive

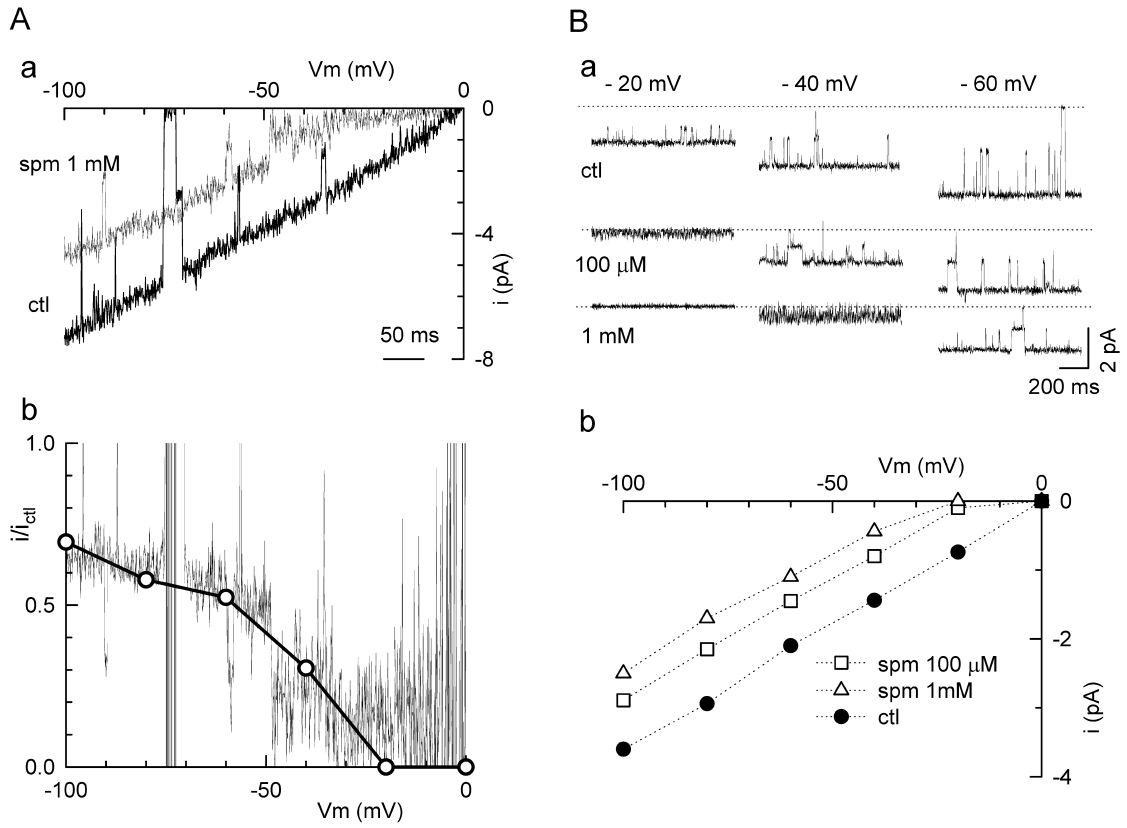

FIGURE 4. Two mechanisms of spermine block at different voltages. (A) Single channel recordings during a voltage ramp from −100 to 0 mV, showing the continuous I-V relationship of a single channel in the absence (control) and presence of 1 mM spermine (a). Currents were filtered at 1 kHz and sampled at 2 kHz. The ratio (i/i_{ctl}) of the two traces in (a) is shown as the noisy thin line in (b). (B) The single channel recordings at test potentials of −20, −40, and −60 mV in the absence and presence of 100 μM and 1 mM spermine (a). At −60 mV (right), the single channel conductance is reduced by spermine without affecting open channel noise. At −40 mV (middle) in the presence of 100 μM spermine, and at −20 mV (left) in the presence of 1 mM spermine, however, open channel noise is increased. The I-V relations are plotted in (b) and the ratio for 1 mM spermine is plotted in A b (open circles), showing good agreement with the ratio obtained from the voltage ramp.

than −50 mV, however, the channels suddenly transited to a state of high open channel noise, consistent with spermine entering more deeply into the pore and causing rapid open channel block. The increased open channel noise under the latter conditions is better seen in the voltage clamps in Fig. 4 B, a. At −60 mV, open channel noise did not increase at either 0.1 or 1 mM spermine, even though single channel current amplitude was progressively reduced as spermine concentration increased. At −40 mV, on the other hand, open channel noise increased significantly at 1 mM spermine, and at −20 mV at 0.1 mM spermine. Fig. 4 A, b shows the ratio of the single channel current amplitude in the presence to that in the absence of 1 mM spermine. The ratio obtained from the voltage ramp (Fig. 4 A, a) agreed well with the data points (open dots) corresponding to the voltage clamps (Fig. 4 B, b) and was very similar to that obtained from macroscopic currents (Fig. 2 C). In summary, this experiment provides evidence at the single channel level for two separable blocking processes by spermine: first, at negative voltages, there was a reduction in single channel current amplitude without increased open channel noise, suggesting that K permeation rate had decreased; and second, with further depolarization, there was an apparent further reduction in single channel current amplitude due to kinetically unresolved rapid open channel block as spermine entered more deeply into and intermittently occluded the pore.

Charge Screening Reduces the Single Channel Current Amplitude of Kir2.1 Channels

It is known that surface potential can affect ion permeation rate through a channel by altering local driving force of permeant ions across the selectivity filter. We postulated that negatively charged residues near the inner vestibule of Kir2.1 might generate such a surface potential as a means of enhancing K permeation rate. The reduction in single channel amplitude by posi-

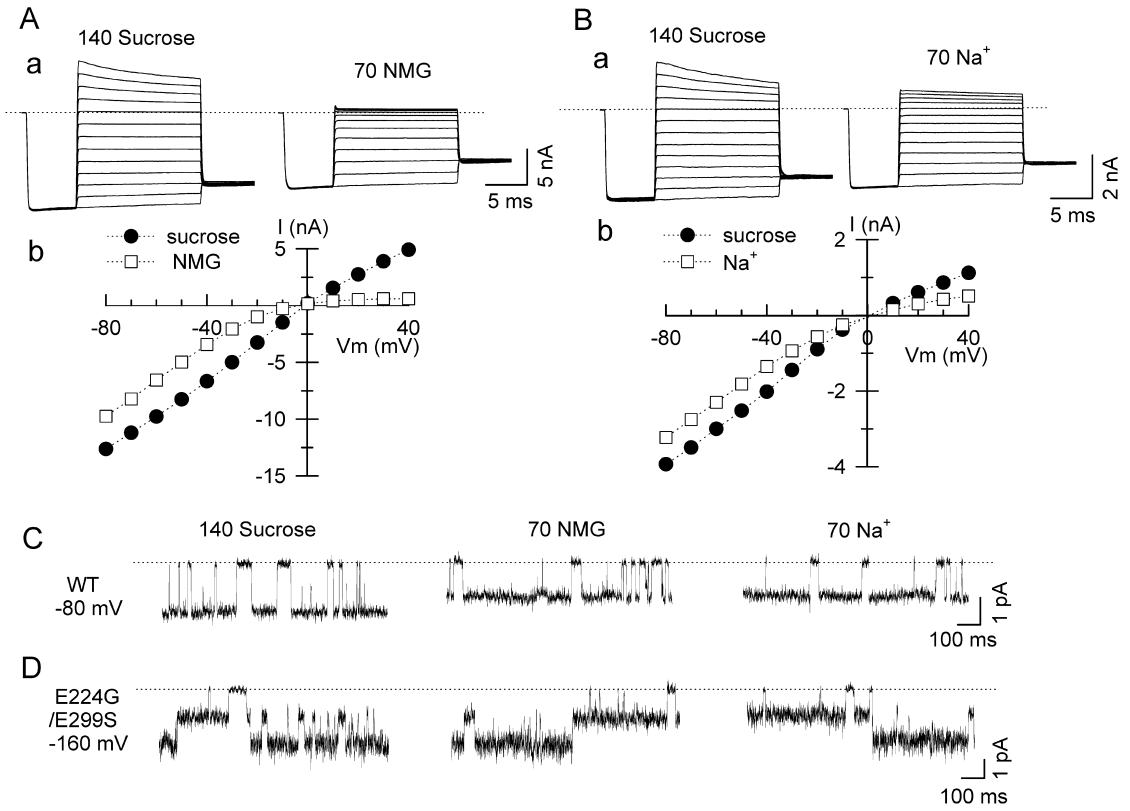

FIGURE 5. Effects of ionic strength on wild-type and mutant Kir2.1 channel currents. Ionic strength was increased by replacing 140 mM sucrose with 70 mM NMG^+ or 70mM Na^+. (A and B) Macroscopic currents (a) of wild-type Kir2.1 channel were recorded with symmetrical 30 mM K in intracellular and extracellular solutions. The macroscopic I-V curves in the presence of sucrose vs. NMG^+ or Na^+ are shown in (b) in both panels. (C) Single channel recording from wild-type Kir2.1 under symmetrical 30 mM K^+ conditions at holding potential of −80 mV. (D) Single channel recording of the double mutant channel E224G/E299S under the same condition at holding potential of − 160 mV. There were two channels in this patch.

tively charged ions such as polyamines might then be explained by their entering the inner vestibule and screening this surface potential. To test this hypothesis, we first examined whether the single channel current amplitude of Kir2.1 channels was affected by a standard intervention known to screen surface potential, namely ionic strength. Fig. 5 A, a shows macroscopic recordings from excised inside-out patches in which the ionic strength of a bath solution containing 30 mM KCl and 140 mM sucrose was increased by replacing sucrose with 70 mM NMG, with bath and pipette $[K^+]$ remaining constant at 30 mM. The I-V relationship shows the macroscopic current amplitude decreased in a voltage-dependent manner similar to spermine (Fig. 5 A, b) when NMG replaced sucrose. Similar results were obtained when sucrose was replaced with 70 mM Na^+ (Fig. 5 B, a and b), although outward current was less strongly affected. We then performed single channel recording under the same condition as in the above macroscopic current experiments. As shown in Fig. 5 C, the unitary amplitude of the single channel was reduced when the ionic strength of the solution was increased by replacing 140 mM sucrose with 70 mM NMG (middle) or 70 mM Na^+ (right) at −80 mV. These findings show that the single channel current amplitude of Kir2.1 channels at negative voltages is reduced when surface potential is screened by changing ionic strength.

If the postulated negative surface charges screened by polyamines or increased ionic strength are located near the inner vestibule of Kir2.1, and if the shallow voltage-dependent component of spermine block (i.e., decrease of the single channel amplitude) is related to its screening these surface charges, then neutralization of these charges via mutagenesis would be predicted to reduce this component of spermine block relative to the steep voltage-dependent component. Although the residues comprising the inner vestibule are not precisely known, several negatively charged residues in the COOH terminus of Kir2.1, specifically E224 and E299, have been shown to regulate polyamine sensitivity (Yang et al., 1995; Kubo and Murata, 2001). From their position, it is plausible that they are located near the inner vestibule. Fig. 5 D shows the single channel record-

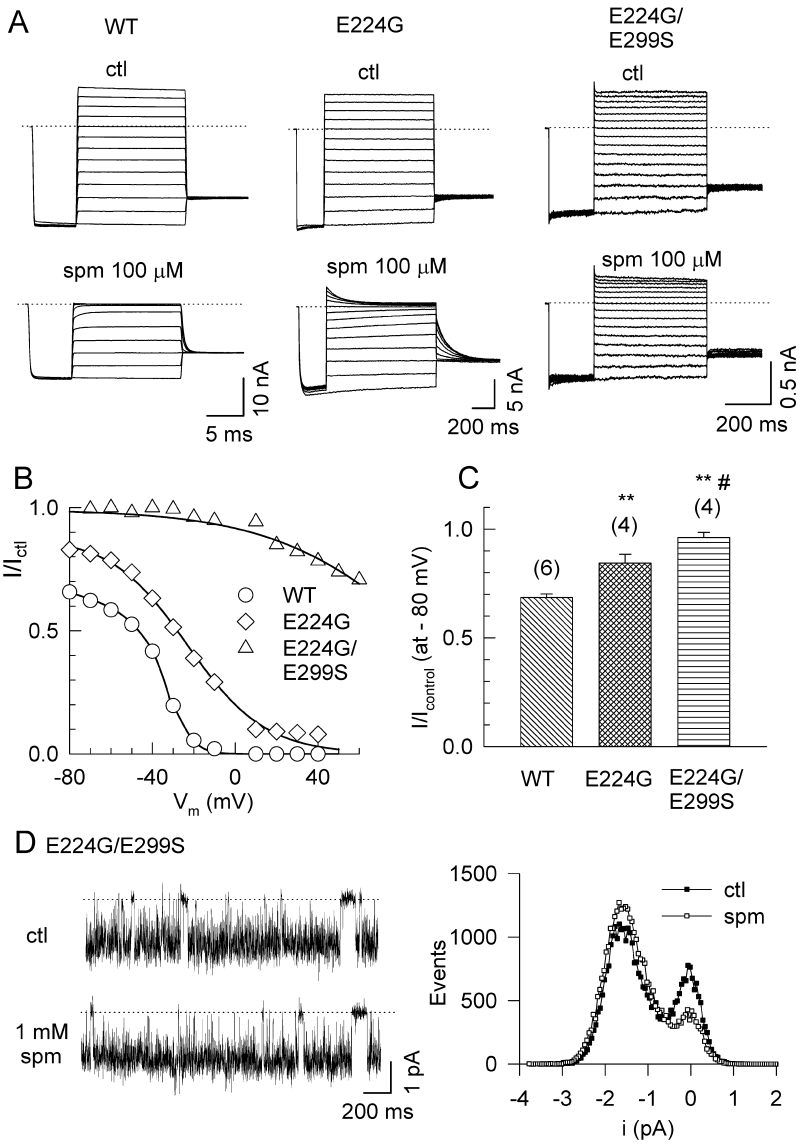

FIGURE 6. Effect of neutralizing E224 and E299 on spermine block. (A) Representative macroscopic current recordings from giant inside-out patches excised from oocytes expressing wild-type Kir2.1 (WT), the mutant E224G, and the double mutant E224G/E299S, in the absence and presence of 100 μM spermine. (B) Ratio of the steady-state current in the presence of spermine to that in its absence (I_{ctl}) vs. voltage for WT, E224G, and E224G/E299S. The smooth lines are fitted value to model 2 in Fig. 8 B. (C) Bar graph comparing the reduction in the macroscopic current amplitude at −80 mV by 100 μM spermine, in WT (n = 6), E224G (n = 4), and E224G/E299S (n = 4). **, $P < 0.05$ compared with WT, and #, $P < 0.05$ compared with E224G. (D) Single channel recording of the double mutant E224G/E299S in the absence (ctl) and presence of 1 mM spermine. The holding potential was at −80 mV. The left panel shows typical single channel current traces and right panel shows superimposed amplitude histograms.

ing of the double mutant channel E224G/E299S, in which these negative charges were neutralized. Unlike wild-type channels, there was no reduction in the single channel amplitude observed when 140 mM sucrose was replaced with 70 mM NMG^+ (middle) or 70 mM Na^+ (right). The recordings were made at −160 mV to better visualize and quantify the single channel currents, since at −80 mV with 30 mM K, single channel currents of the double mutant were very noisy due to its smaller single channel conductance and rapid flickery kinetics, as described previously by Yang et al. (1995) and Kubo and Murata (2001). In giant patches from oocytes expressing the double mutant, macroscopic currents increased when ionic strength was enhanced, possibly due to effects on channel gating given the lack of change in single channel conductance.

Fig. 6 shows the effects of spermine on macroscopic currents in the Kir2.1 single mutant E224G and the double mutant E224G/E299S. Compared with wild-type channels, spermine sensitivity was lower as reported previously (Yang et al., 1995; Kubo and Murata, 2001). Moreover, the shallow voltage-dependent component of spermine block was reduced in E224G and nearly eliminated in E224G/E299S (Fig. 6, B and C). Consistent with the ionic strength experiments, in the E224G/E299S double mutant channel, 1 mM spermine had no effect on the single channel current amplitude (which could be resolved at −80 mV with symmetrical 100 mM K) (Fig. 6 D). These findings support the hypothesis that these residues are located near the inner vestibule and contribute negative surface potential which regulates the permeation rate of K ions through the pore.

The negatively charged residue D172, which is also know to be crucial for polyamine or Mg^{2+} block (Lu and MacKinnon, 1994; Stanfield et al., 1994; Wible et

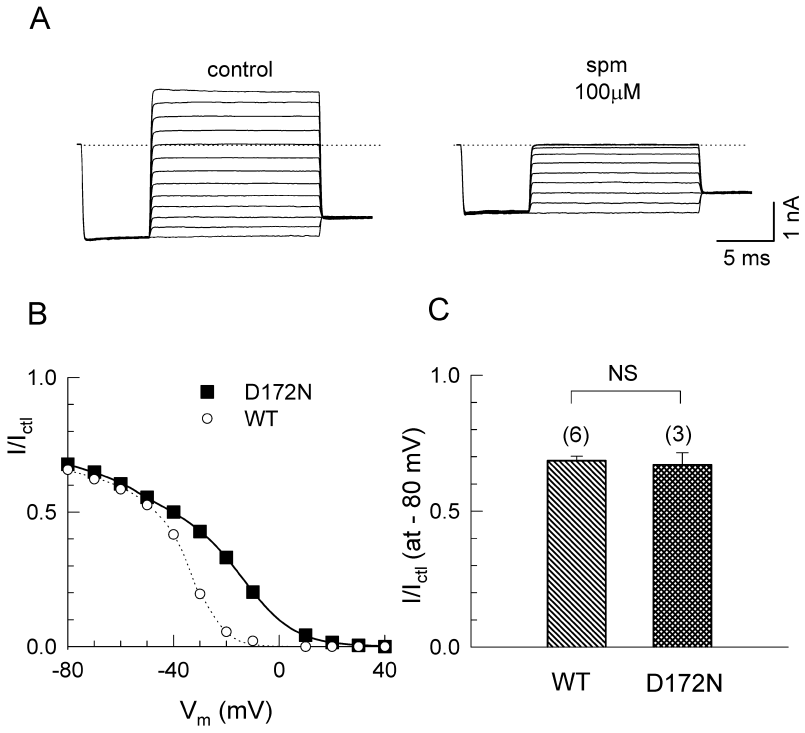

FIGURE 7. Effect of neutralizing D172 on spermine block. (A) Representative macroscopic current recordings from oocytes expressing wild-type and D172N channels in the absence and presence of 100 μM spermine. (B) Ratio of the steady-state current in the presence of spermine (I) to that in its absence (I_{ctl}) vs. voltage for WT (the same values as Fig. 6 B) and D172N. The smooth lines are fitted value to model 2 in Fig. 8 B. (C) Bar graph comparing the reduction in the currents at −80 mV by 100 μM spermine, in WT ($n = 6$), D172N ($n = 3$).

al., 1994; Yang et al., 1995), is thought to be located deep in the channel pore and therefore would not necessarily contribute to surface charge in the inner vestibule. Consistent with these predictions, Fig. 7 shows that neutralization of D172 had no effect on the shallow charge screening component of spermine block at −80 mV, whereas it did significantly affected the pore block component at −20 mV.

A Quantitative Model of Spermine Block of Kir2.1 Incorporating Surface Charge–screening Effects

The most difficult feature to account for in the pattern of block of Kir2.1 by spermine is the shallow voltage-dependent component of block (Fig. 2), since the dose-response curve for spermine block has a Hill coefficient of ~0.3 at voltages greater than −60 mV. Although this low Hill coefficient could be explained by allosteric effects of spermine on channel open probability, when we examined the effects of spermine on channel open probability we found no significant change. Instead, we observed that spermine decreased the single channel current amplitude in a concentration- and voltage-dependent fashion. It is possible to reproduce a Hill coefficient <1 if partial conductance states are allowed.

To develop a quantitative model, we started with a two open state (O_0, O_1), one blocked state (B) linear reaction scheme, as proposed recently by Kubo and Murata (2001). However, we assigned a fractional conductance g (a function of both voltage and spermine concentration) to the conductance of the O_1 state, to represent the charge-screening effect of spermine on single channel amplitude (Fig. 8 B, Model 1).

Since it is not possible to predict g from first principles without knowing the precise molecular topology of the inner vestibule, we used a completely empirical approach to model the putative surface charge–screening effect. We defined g as the ratio (i/i_0) of the current in the presence (i) and absence (i_0) of spermine using the single channel I-V curve as in Fig. 4 A. In both the single channel and macroscopic data, spermine shifted the I-V curves at negative voltages to the left while maintaining the same slope (Fig. 2 B and Fig. 4 A, a), such that the extrapolation of the I-V curve in the presence of spermine intersected the voltage axis at V_T, as illustrated in Fig. 8 A, a. We measured V_T for different spermine concentrations, and fit the results to a Hill equation $V_T = V_{T,max}/(1+(Kd/[spm])^n$, where $V_{T,max}$ is the value of V_T achieved at saturating spermine concentration. We also assumed that at a given spermine concentration, there was a voltage Vg_{min} beyond which all of the negative surface charge was maximally screened such that $g = g_{min}$ remained constant thereafter. Thus:

$$\text{for } V > Vg_{min}, \qquad g = g_{min}. \tag{1}$$

At voltages negative to Vg_{min}, the slopes (s) of the I-V curves in the presence and absence of spermine were identical, so that:

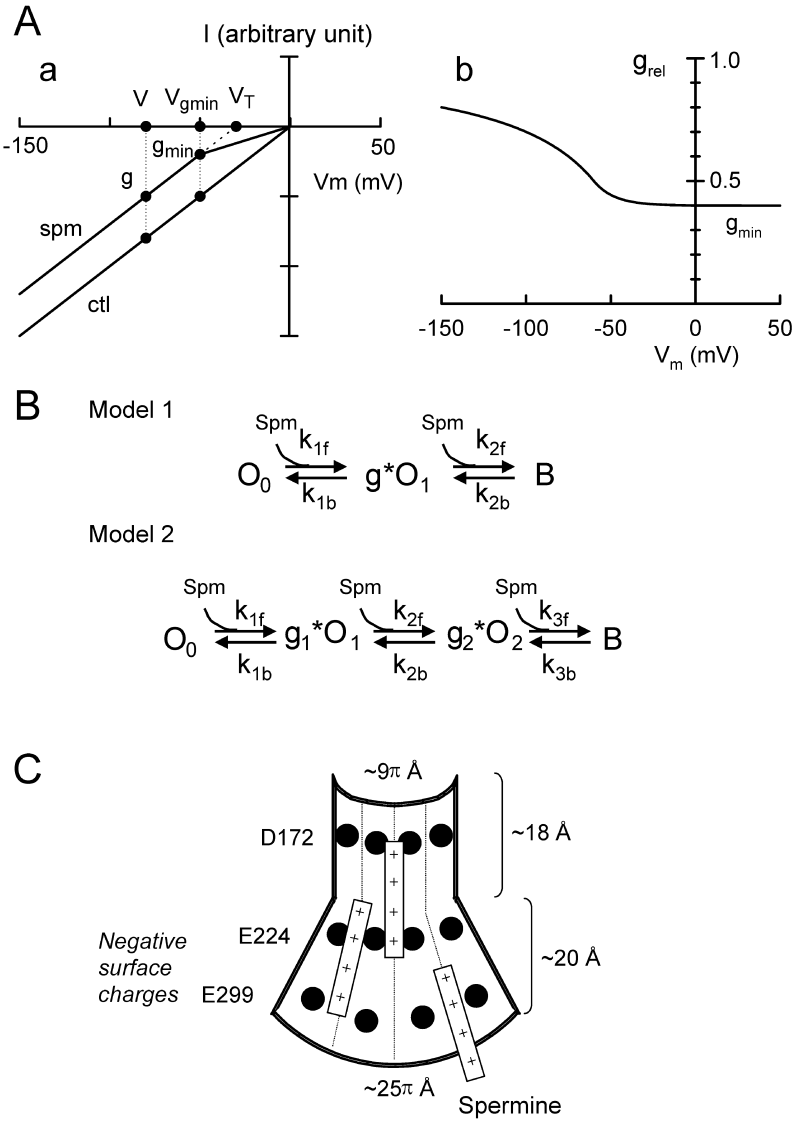

FIGURE 8. Proposed model for spermine block of Kir2.1 current. (A) Empirical method to obtain fractional reduction in single channel conductance due to charge-screening by spermine. A a shows superimposed I-V curves in the presence (spm) and absence (ctl) of spermine. A b shows the voltage dependence of the relative conductance (g_{rel}) obtained from the ratio of the single channel current amplitude in the presence and absence of spermine in a. See text for details. (B) Reaction schemes for models used to fit the results, with g representing the fractional conductance of open state(s) due to charge-screening by spermine. (C) Schematic representation of the inner vestibule of Kir2.1, cut open from its conical shape to form a sheet. Putative locations of D172, E224, and E299 as indicated, with examples of spermine molecules bound electrostatically at various depths.

$$\text{for } V > Vg_{min}, \qquad (2)$$
$$g = i/i_o = s(V - V_T)/sV = (V - V_T)/V.$$

The relationship between g and V obtained using this approach is shown in Fig. 8 A, b. To avoid an indeterminate slope of this curve at $V = Vg_{min}$, we smoothed the joining of the two segments in Eqs. 1 and 2 with an exponential decay beginning at $V = Vg_0 - 10$ mV. This only affected g modestly over a 10 mV range. The fit of Model 1 (Fig. 8 B) to the data was only fair, but was considerably improved by introducing an additional partially conducting open state (O_2) (Fig. 8 B, Model 2), using the analogous approach outlined above for obtaining g_1 and g_2. Fig. 9 shows the fitting results. Both the voltage dependence of the steady-state current (Fig. 9 A) and the kinetics of spermine block (Fig. 9 B, a) and unblock (Fig. 9 B, b) were well fitted by Model 2. For the surface charge screening effects of spermine, the values of g_{min1} and g_{min2} are 0.61 ± 0.07 and 0.43 ± 0.09, respectively. They have higher affinity (K_{d1} = 1.4 [± 0.5] × 10^{-6} M; K_{d2} = 9.2 [± 3.0] × 10^{-6} M) but shallower voltage dependence (Z_1 = 0, Z_2 = 3.0 ± 0.1) than the pore block by spermine (K_{d3} = 4.3 [± 0.9] × 10^{-4} M, Z_3 = 4.5 ± 0.1). The forward (f) and backward (b) rate constants for the three transitions are: k_{1f} = 1.1 (± 0.4) × 10^{12} $M^{-1}s^{-1}$, k_{1b} = 1.7 1 (± 0.8) × 10^7 s^{-1}, k_{2f} = 3.5 (± 1.5) × 10^{12} $M^{-1}s^{-1}$, k_{2b} = 3.5 (± 2.4) × 10^6 s^{-1}, k_{3f} = 4.8 (± 2.6) × 10^6 $M^{-1}s^{-1}$ and k_{3b} = 1.6 (± 0.5) × 10^3 s^{-1} (n = 3). All K_d, k_f, and k_b values were calculated relative to −40 mV, with voltage dependence described by $K_{(V)} = K_{(-40)}\exp(-ZFV/RT)$.

Fig. 6 C also shows the fit of this model to the steady-state I-V curve for the E224G and E224G/E299S mutants, respectively. Consistent with the idea that these mutations reduce negative surface potential near the

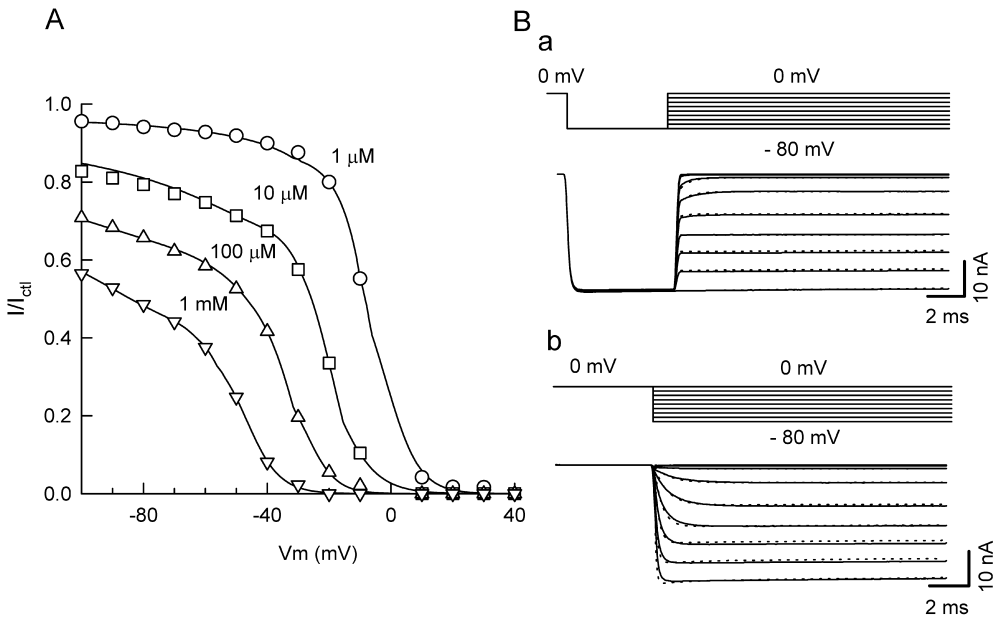

FIGURE 9. Fitting model 2 to experimental data. (A) Family of steady-state I-V relationships in the presence of the spermine concentrations indicated. Points are experimental data taken from Fig. 2 C, and lines show the best fit of the model. The parameters determined from the fits are: $g_{01} = 0.48$, $g_{02} = 0.28$, $K_{d1} = 5.4 \times 10^{-7}$ M; $K_{d2} = 1.48 \times 10^{-5}$ M, $K_{d3} = 4.3 \times 10^{-4}$, $Z_1 = 0$, $Z_2 = 3.1$, $Z_3 = 4.4$. (B) Kinetics of Kir2.1 current block (a) and unblock (b) in the presence of 100 μM spermine using the voltage protocols shown. Points are the experimental data, with best fit of the model shown as superimposed lines. The forward (f) and backward (b) rate constants for the three transitions determined from fit in this patch are: $k_{1f} = 2.6 \times 10^{12}$ $M^{-1}s^{-1}$, $k_{1b} = 1.4 \times 10^{6}$ s^{-1}, $k_{2f} = 5.7 \times 10^{12}$ $M^{-1}s^{-1}$, $k_{2b} = 8.4 \times 10^{7}$ s^{-1}, $k_{3f} = 2.4 \times 10^{6}$ $M^{-1}s^{-1}$ and $k_{3b} = 1.2 \times 10^{3}$ s^{-1}.

inner vestibule so that there is less for spermine to screen, a major change in the fitting parameters involved increases in the values of g_{min1} and g_{min2} as 0.89 ± 0.03 and 0.87 ± 0.04 in E224G, and to 0.97 ± 0.01 and 0.97 ± 0.01 in E224G/E299S mutant (i.e., reflecting a reduced ability of spermine to decrease single channel current amplitude of the O_1 and O_2 states). Also, the new values of k_{1f} (5.8 [± 1.3] $\times 10^9$ $M^{-1}s^{-1}$) and k_{2f} (9.9 [± 4.5] $\times 10^9$ $M^{-1}s^{-1}$) were over 100-fold slower than in wild-type channels (see DISCUSSION). In addition, there was a reduction in the voltage dependence of the $g_2O_2 \leftrightarrow B$ transition (K_3), with Z_3 decreasing from 4.5 ± 0.1 to 1.5 ± 0.1 in E224G and to 0.6 ± 0.1 in E224G/E299S, respectively. These results could suggest that tethering of spermine to E224 and/or E299 may resist its entry deeper into the pore, thereby steepening its voltage dependence.

For the D172N mutation, on the other hand, the fitted values of g_{min1} and g_{min2} were 0.58 ± 0.02 and 0.36 ± 0.03, respectively, in the same range as in wild-type channel. The affinity and the voltage dependence of the pore-blocking effect ($K_{d3} = 4.2$ [± 2.0] $\times 10^{-3}$ M, $Z_3 = 3.2 \pm 0.4$), however, were reduced, consistent with D172's involvement exclusively in pore block by spermine, rather than surface charge effects.

To test the robustness of model 2, we also calculated the concentration of spermine predicted to cause half-maximal block (IC_{50}) at 40 mV using the same parameter values. The IC_{50} values averaged 6.1 ± 0.6 nM for WT and 2.8 ± 0.3 μM for E224G, in good agreement with previous experimental measurements (Lee et al., 1999).

DISCUSSION

In the present study, we examined the block of Kir2.1 channels by spermine over a physiological concentration range, both at the macroscopic and single channel current level. The results show that spermine blocks Kir2.1 channels by two distinct mechanisms: first by reducing single channel amplitude at negative voltages, which we attribute to charge-screening effects, and then by direct open channel block as membrane potential is depolarized. A quantitative model is proposed which accounts for both steady-state and kinetic features of the complex voltage and concentration dependence of spermine block.

Surface Charge–screening Component of Spermine Block

It is well recognized that charged groups on channel proteins and nearby lipids can influence channel behavior by generating local surface potentials. The effects of surface charge on channel gating have been studied extensively, but effects on ion permeation have been less thoroughly characterized. In principle, surface potentials can affect both gating and permeation in voltage-sensitive channels (MacKinnon et al., 1989; Zhou and Jones, 1995). For gating, it has been assumed that a surface potential (Φ) simply shifts the probability that a channel will undergo a gating transition along the voltage axis by Φ mV. Effects of surface potentials on permeation are more complex, as two effects are predicted. First, the local voltage profile seen by an ion as it moves through rate-limiting step in permeation (i.e., movement through the selectivity filter) is shifted by surface

potential, thereby influencing the permeation rate, although not the reversal potential. Second, a surface potential may alter the local concentration of the permeant ion in the inner or outer vestibule of the channel.

In the case of Kir2.1 channel, we can apply Gouy-Chapman theory (Hille, 2001) and recent structural information (Doyle et al., 1998; Lu et al., 1999a,b; Guo and Lu, 2001) to crudely estimate what the surface potential (Φ) might be in the Kir2.1 inner vestibule. Fig. 8 C shows a schematic representation, with the Kir2.1 inner vestibule cut open to form a sheet with the negative surface charges at E299, E224, D172, as indicated. Multiple spermine molecules are presumed to simultaneously enter the inner vestibule to screen E224 and/or E229 at different levels as illustrated. The diameter of the selectivity filter end of the inner vestibule has been measured at 9 Å and extends toward the cytoplasm for a distance of 18 Å (Doyle et al., 1998; Guo and Lu, 2001). If we assume that the inner vestibule subsequently expands to a diameter of 25 Å at its cytoplasmic end for a distance of 20 Å (Lu et al., 1999a,b), the total inner vestibule surface area is ~1633 Å^2. With each of four subunits contributing two charges at E224 and E299, this would correspond to a surface charge density (σ) of 1 charge/204 Å^2. Using the Grahame equation:

$$\sigma^2 = 2\varepsilon\varepsilon_0 RT\Sigma C_i[\exp(-z_i F\Phi/RT)-1]$$

where z_i is the valence of the i^{th} ion species, C_i is the concentration of the i^{th} ion in the bulk solution, ε is the dielectric constant for aqueous solution, ε_0 is the permitivity of free space, and F, R, and T have their normal meaning (for review see Hille, 2001), this would create a surface potential Φ of ~75 mV. To relate this to ion permeation rate, the simplest description for ion permeation is the Goldman-Hodgkin-Katz (GHK) equation, in which the ion permeation rate is directly proportional to the driving force. At −60 mV, for example, the local driving force and hence single channel amplitude would decrease by >50% if the surface potential arising from E224 and E299 were fully screened. Although this estimate is very crude and subject to a number of unrealistic simplifying assumptions, it nevertheless illustrates the plausibility that surface charge screening by spermine could have quantitatively important effects on single channel current amplitude, of the same order of magnitude as was observed experimentally. However, accurate calculation of local surface potential in the Kir2.1 inner vestibule from first principles is not feasible without detailed structural knowledge of the local molecular topology. The experiments in which ionic strength was altered also support our hypothesis that single channel amplitude in Kir2.1 channels is sensitive to local surface potential effects. Multivalent cations are even more effective surface charge screeners, but their potent pore-blocking effects on Kir2.1 precluded their use. Similar reductions in inward current amplitude were obtained using Na^+ and NMG^+, indicating that the inner vestibule is wide enough to accommodate the larger NMG^+ molecule. This is consistent with the ability of spermine, also a relatively large molecule, to fit into the inner vestibule to screen surface charges. Cysteine mutagenesis experiments also have shown previously that the inner vestibule of Kir2.1 channel is wide enough to allow multiple successive reactions with large methanethiosulfonate reagents (Lu et al., 1999b). Thus, it is likely that the inner vestibule of Kir2.1 is much wider than an extended polyamine and could allow several polyamines to enter simultaneously, as originally suggested by Yang et al. (1995). In contrast to NMG^+, Na^+ had less effect on outward current (Fig. 5 B). This is consistent with NMG^+ causing open channel block of outward currents, as has been noted previously with other large cations (Guo and Lu, 2001).

Finally, it has also been reported previously that the neutralization of E224 or E299 leads to a reduced unitary conductance (Yang et al., 1995; Kubo and Murata, 2001), consistent with this residue playing a role in surface charge enhancement of K ion permeation in Kir2.1. Our finding that neutralization of E224 and E299 led to a reduction in the shallow voltage-dependent component of spermine block (Fig. 6) fits well with the putative role of these residues contributing to the negative surface potential near the inner vestibule which enhances K ion throughput.

In the model, we needed two open states O_1 and O_2 with reduced conductances (g_1 and g_2) and different voltage dependences (Z_1 and Z_2) to fit the data (Fig. 8 B, Model II). These two states may represent the effects of charge screening at different levels corresponding to E299 and E224 in the inner vestibule. For example, if E299 is essentially outside the transmembrane field, binding of a spermine to this residue may correspond to the O_1 screening effect with the trivial voltage dependence. Conversely, E224 may be in the transmembrane voltage field and correspond to the voltage-dependent O_2 screening effect upon spermine binding. Since there are four charges on spermine, spermine molecules could potentially bind at a variety of levels to any of the eight E299 and E224 residues, producing a variable amount of charge screening by binding (see below).

An interesting observation is that neutralization of E224 led to a marked slowing in both blocking and unblocking kinetics by spermine (Fig. 6). This suggests that E224 enhances spermine's accessibility kinetically to move deeper into the pore to occlude K permeation, and may also facilitate its exit from the pore blocking

site. In this regard, the forward rate constants K_{1f} and K_{2f} in the model for the first two steps (the charge-screening effect) are considerably higher ($10^{12–13}$ $M^{-1}s^{-1}$) than expected for binding reactions in which 10^8 $M^{-1}s^{-1}$ is generally considered the diffusion limit for molecules in solution (Hille, 2001). However, these rate constants incorporate the bulk spermine concentration in their calculation, and this may grossly underestimate the local spermine concentration near the inner vestibule due to the substantial negative surface potential in this region (a surface potential of −60 mV would concentrate local spermine by as much as four orders of magnitude). In the E224G mutant, the fitted values of K_{1f} and K_{2f} were reduced by >100-fold, consistent with reduced spermine accumulation locally near the inner vestibule via this postulated mechanism.

Screening Versus Tethering

Surface charge screening may or may not involve a specific binding interaction between the surface charge and the screening counterion. The present results do not indicate whether screening of inner vestibule negative surface charges by spermine or other blockers involves screening alone, or screening plus binding. However, the very slow time course of the increase in single channel amplitude when spermine was washed out (Fig. 3 A, a) may suggest that spermine binds nonocclusively to E224 and E299 in the inner vestibule. Buffering of spermine by other negative charges in the protein or surrounding lipids may also occur and contribute to its slow washout. Spermine washout certainly did not appear too diffusion-limited, however, since TEA washout under the same conditions was much more rapid.

Spermine binding to residues such as E224 and/or E299 does not contradict the apparently continuous increase in single channel amplitude during spermine washout. If we assume that more than one spermine molecule can occupy the inner vestibule simultaneously without occluding the pore, and that each spermine molecule can bind at any one of its four positive charges to any one of eight negative charges in the inner vestibule (see schematic in Fig. 8 C), then the number of possible binding configurations are 8, 36, and 120 for one, two, or three spermine molecules, respectively. In this calculation, we have counted only symmetrically distinct conformations in which the spermine molecules are located at different depths as a result of their tethering by E224 or E299, irrespective of the specific subunit. Each of these conformations therefore potentially represents a unique degree of surface potential screening, and therefore a unique single channel amplitude. It is clear this large number of combinations for two or more spermine molecules in the inner vestibule would not be resolvable experimentally, and would appear as a continuous change in single channel amplitude, as seen in Fig. 4 A.

Another outcome of postulating that surface charge screening involves binding is that it provides a potential explanation for subconductance levels with other cationic blockers such as Mg^{2+} and Cs^+ observed in previous single channel studies in Kir2.1 (Matsuda et al., 1987, 1989; Mazzanti et al., 1996; Oishi et al., 1998). These previously described cation-induced discrete subconductance states may be caused by similar charge-screening effects as occur with spermine, rather than representing true conformational changes of the channel pore. In contrast to spermine, Mg^{2+} and Cs^+ do not have the linear structure with the extended charge distribution of a polyamine. Thus, if bound to an inner vestibule residue, they would screen a fixed amount of the surface charge. For example, if Mg^{2+} were to bind only to E224 at either one, two, or three subunits, this would produce three discrete subconductance states, as have been observed experimentally, rather than an apparent continuum like spermine. Channels partially modified by MTS reagents also exhibited distinct subconductance levels (Lu et al., 1999a). In this study, cationic MTS reagents may also have induced subconductance states by screening fixed increments of negative surface charge near the inner vestibule in proportion to the number of subunits labeled with cysteine.

Finally, a recent study reported that the unitary conductance of both expressed Kir2.1 channels or and native I_{K1} channels in cardiac myocytes formed a broad distribution, ranging from 2 to 33 pS (Picones et al., 2001). It is interesting to speculate that this variability might be related to differences in the degree of surface charge screening in the inner and/or outer vestibules. If so, this raises the possibility that Kir2.1 single channel conductance may be regulated physiologically by this mechanism.

Pore Block Component of Spermine Block

In the present study, we have also demonstrated for the first time at the single channel level that spermine acts as a very fast open channel blocker as membrane voltage is progressively depolarized. The rapid transition between open and blocked states as seen in Fig. 4, A and B, is consistent with the idea that spermine is concentrated locally near the inner vestibule, facilitating its rapid movement to and from its occlusive site in the pore (putatively at D172). This result agrees with Kubo and Murata (2001) and also with our finding that the kinetics of spermine block and unblock become markedly slower when E224 is neutralized (Fig. 6). It is also notable that the valence of the $O_2 \leftrightarrow B$ step was 4.5, greater than the total charge move-

ment for one spermine molecule traversing the full distance across the transmembrane voltage field. Sweeping out of K^+ ions from the channel pore when spermine moves into its blocking position deep in the pore may explain this extra charge movement (Pearson and Nichols, 1998).

We thank Dr. L.Y. Jan for providing the Kir2.1 clone, and Y. Lu for technical support. We thank R. Olcese, E. Stefani, F. Bezanilla, Z. Qu, and K. Phillipson for valuable discussions.

This work was supported by National Institutes of Health R37 HL60025 (to J.N. Weiss), by an American Heart Association, Western States Affiliate Postdoctoral Fellowship (to L.-H. Xie) and by the Kawata and Laubisch Endowments.

Submitted: 7 February 2002
Revised: 21 May 2002
Accepted: 21 May 2002

REFERENCES

Doupnik, C.A., N. Davidson, and H.A. Lester. 1995. The inward rectifier potassium channel family. *Curr. Opin. Neurobiol.* 5:268–277.

Doyle, D.A., J. Morais Cabral, R.A. Pfuetzner, A. Kuo, J.M. Gulbis, S.L. Cohen, B.T. Chait, and R. MacKinnon. 1998. The structure of the potassium channel: molecular basis of K+ conduction and selectivity. *Science.* 280:69–77.

Fakler, B., U. Brandle, E. Glowatzki, S. Weidemann, H.P. Zenner, and J.P. Ruppersberg. 1995. Strong voltage-dependent inward rectification of inward rectifier K^+ channels is caused by intracellular spermine. *Cell.* 80:149–154.

Ficker, E., M. Taglialatela, B.A. Wible, C.M. Henley, and A.M. Brown. 1994. Spermine and spermidine as gating molecules for inward rectifier K^+ channels. *Science.* 266:1068–1072.

Guo, D., and Z. Lu. 2001. Kinetics of inward-rectifier K+ channel block by quaternary alkylammonium ions. dimension and properties of the inner pore. *J. Gen. Physiol.* 117:395–406.

Hille, B. 2001. Ionic Channels of Excitable Membranes. 3rd ed. Sinauer Associates, Inc. Sunderland, MA. 814 pp.

Ho, S.N., H.D. Hunt, R.M. Horton, J.K. Pullen, and L.R. Pease. 1989. Site-directed mutagenesis by overlap extension using the polymerase chain reaction. *Gene.* 77:51–59.

Kubo, Y., T.J. Baldwin, Y.N. Jan, and L.Y. Jan. 1993. Primary structure and functional expression of a mouse inward rectifier potassium channel. *Nature.* 362:127–133.

Kubo, Y., and Y. Murata. 2001. Control of rectification and permeation by two distinct sites after the second transmembrane region in Kir2.1 K+ channel. *J. Physiol.* 531:645–660.

Lee, J.-K., S.A. John, and J.N. Weiss. 1999. Novel gating mechanism of polyamine block in the strong inward rectifier K channel Kir2.1. *J. Gen. Physiol.* 113:555–564.

Lopatin, A.N., E.N. Makhina, and C.G. Nichols. 1994. Potassium channel block by cytoplasmic polyamines as the mechanism of intrinsic rectification. *Nature.* 372:366–369.

Lopatin, A.N., E.N. Makhina, and C.G. Nichols. 1995. The mechanism of inward rectification of potassium channels: "long-pore plugging" by cytoplasmic polyamines. *J. Gen. Physiol.* 106:923–955.

Lu, Z., and R. MacKinnon. 1994. Electrostatic tuning of Mg2+ affinity in an inward-rectifier K+ channel. *Nature.* 371:243–246.

Lu, T., B. Nguyen, X. Zhang, and J. Yang. 1999a. Architecture of a K^+ channel inner pore revealed by stoichiometric covalent modification. *Neuron.* 22:571–580.

Lu, T., Y.G. Zhu, and J. Yang. 1999b. Cytoplasmic amino and carboxyl domains form a wide intracellular vestibule in an inwardly rectifying potassium channel. *Proc. Natl. Acad. Sci. USA.* 96:9926–9931.

MacKinnon, R., R. Latorre, and C. Miller. 1989. Role of surface electrostatics in the operation of a high-conductance Ca2+-activated K+ channel. *Biochemistry.* 28:8092–8099.

Matsuda, H., A. Saigusa, and H. Irisawa. 1987. Ohmic conductance through the inwardly rectifying K channel and blocking by internal Mg^{2+}. *Nature.* 325:156–159.

Matsuda, H., H. Matsuura, and A. Noma. 1989. Triple-barrel structure of inwardly rectifying K+ channels revealed by Cs+ and Rb+ block in guinea-pig heart cells. *J. Physiol.* 413:139–157.

Mazzanti, M., R. Assandri, A. Ferroni, and D. DiFrancesco. 1996. Cytoskeletal control of rectification and expression of four substates in cardiac inward rectifier K+ channels. *FASEB J.* 10:357–361.

Oishi, K., K. Omori, H. Ohyama, K. Shingu, and H. Matsuda. 1998. Neutralization of aspartate residues in the murine inwardly rectifying K+ channel IRK1 affects the substate behaviour in Mg^{2+} block. *J. Physiol.* 510:675–683.

Pearson, W.L., and C.G. Nichols. 1998. Block of the Kir2.1 channel pore by alkylamine analogues of endogenous polyamines. *J. Gen. Physiol.* 112:351–363.

Picones, A., E. Keung, and L.C. Timpe. 2001. Unitary conductance variation in Kir2.1 and in cardiac inward rectifier potassium channels. *Biophys. J.* 81:2035–2049.

Shieh, R.C., S.A. John, J.K. Lee, and J.N. Weiss. 1996. Inward rectification of the IRK1 channel expressed in Xenopus oocytes: effects of intracellular pH reveal an intrinsic gating mechanism. *J. Physiol.* 494:363–376.

Stanfield, P.R., N.W. Davies, P.A. Shelton, M.J. Sutcliffe, I.A. Khan, W.J. Brammar, and E.C. Conley. 1994. A single aspartate residue is involved in both intrinsic gating and blockage by Mg2+ of the inward rectifier, IRK1. *J. Physiol.* 478:1–6.

Taglialatela, M., E. Ficker, B.A. Wible, and A.M. Brown. 1995. C-terminus determinants for Mg^{2+} and polyamine block of the inward rectifier K^+ channel IRK1. *EMBO J.* 14:5532–5541.

Vandenberg, C.A. 1987. Inward rectification of a potassium channel in cardiac ventricular cells depends on internal magnesium ions. *Proc. Natl. Acad. Sci. USA.* 84:2560–2564.

Wible, B.A., M. Taglialatela, E. Ficker, and A.M. Brown. 1994. Gating of inwardly rectifying K+ channels localized to a single negatively charged residue. *Nature.* 371:246–249.

Yang, J., Y.N. Jan, and L.Y. Jan. 1995. Control of rectification and permeation by residues in two distinct domains in an inward rectifier K^+ channel. *Neuron.* 14:1047–1054.

Zhou, W., and S.W. Jones. 1995. Surface charge and calcium channel saturation in bullfrog sympathetic neurons. *J. Gen. Physiol.* 105:441–462.